Smart PV Hydroponic Greenhouse for Sustainable Agriculture in Tunisia

Rym Marouani
Laboratory of ATSSEE, Faculty of Sciences of Tunis, University of Tunis El Manar, Tunisia
rym.marouani@fst.utm.tn (corresponding author)

Chabakata Mahamat
UMR Espace-Dev, University of French Guiana, French Guiana
chabakata.mahamat@univ-guyane.fr

Sofiane Khachroumi
Higher Institute of Information and Communication Technologies, Tunisia
sofianekha204@gmail.com

Salwa Bouadila
Center for Research and Energy Technologies, Tunisia
salwa.bouadila@crten.rnrt.tn

Adnen Cherif
Laboratory of ATSSEE, Faculty of Sciences of Tunis, University of Tunis El Manar, Tunisia
adnane.cherif@fst.utm.tn

Received: 18 March 2024 | Revised: 2 April 2024 | Accepted: 8 April 2024

 DOI: https://doi.org/10.48084/etasr.7278

ABSTRACT

This study introduces smart tools and algorithms for controlling and monitoring Sustainable Agricultural Greenhouses (SHG). Through the implementation of solar energy, Internet of Things (IoT) sensor-actuator networks, and artificial intelligence, an SHG with a low carbon footprint has been designed. The former makes minimal use of water resources, resulting in the reduction of costs while optimizing crops and harvests. After choosing the structure and architecture of the system introduced, optimized PID controllers based on Artificial Neural Networks (ANN) are proposed, for the maximum power to be derived from the Photovoltaic (PV) solar source and the efficiency of the pump to be improved. Additionally, an IoT-based remote control system has been created using an ESP32 microcontroller with a Wi-Fi interface along with sensors for monitoring solar irradiation, soil moisture, indoor temperature, humidity, lighting, ventilation, and water flow. The system collects sensor data in real-time and employs a built-in algorithm to update the information in the cloud. The experimental measurements carried out in the SHG allowed for the verification of the chosen models and simulation results. Thanks to the hybridization of renewable energies, hydroponic techniques, smart technologies, and sustainable practices, this cutting-edge greenhouse creates an ideal microclimate for year-round cultivation while preserving the ecosystem's energy and water resources.

Keywords-hydroponic greenhouse; smart PV system; ANN-based PID controller; indirect field oriented control; IoT-based remote control

I. INTRODUCTION

Tunisia's energy policy has focused on achieving self-sufficiency and security while ensuring high-quality service delivery. The policy has also emphasized research and development in exploring non-conventional sources of energy production [1, 2]. Consequently, renewable energy sources have received special attention for a considerable amount of time. Among them, PV energy has emerged as the most popular choice thanks to the advancements in power electronics and computing, [3]. This renewable energy source has a wide coverage area and presents a cost-efficient solution for diverse industrial, space, agriculture and residential applications. Thus, PV energy sources have gained immense popularity due to their versatility and efficiency. The recent developments in this

area are significant and generate considerable benefits with respect to social, environmental, and economic factors [3]. Among the most reliable and cost-effective applications of PV are the grid-connected PV systems [4, 5] and the PV water-pumping systems [6, 7]. Grid-connected PV systems are designed to supply electricity to the grid, while PV water-pumping systems use solar energy to pump water from wells or other places [8]. The latter in particular, utilize different types of motors to drive the water pump, such as permanent magnet, induction and synchronous reluctance motors. Among these, induction motors are considered optimal due to their robust construction, which ensures a dependable, trouble-free, and efficient solar PV water pumping system [9]. The performance of an Induction Motor (IM) is highly dependent on its control. For speed-control drive systems based on IM, the vector-control technique is preferred. In that regard, the field orientation scheme can be classified into two main categories: Direct Field-Oriented Control (DFOC) and Indirect Field-Oriented Control (IFOC) methods. For induction motor drives, the IFOC is the preferred method in industries due to its simplicity [10].

On the other hand, PV water-pumping systems are gaining popularity in agricultural settings due to their ability to efficiently and sustainably provide water for irrigation [11] and greenhouse applications [12], making it a cost-effective and environmentally friendly option for farmers and growers. One of the most significant applications of these systems can be detected in hydroponic greenhouses, where they can play a crucial role in ensuring the optimum growth and yield of crops. Hydroponic greenhouses rely on a controlled environment where plants are grown in a nutrient-rich water solution instead of soil [13]. The PV water pumping system facilitates the circulation of the water solution through the hydroponic greenhouse, ensuring that the plants receive an adequate supply of water, nutrients, and oxygen [14]. Moreover, PV water-pumping systems can assist in the regulation of any indoor environment where plants grow [15].

The suggested application can significantly contribute to sustainable agriculture by reducing water consumption, optimizing crop production, and minimizing the use of harmful chemicals. In [16], the authors provide a detailed review of solar water pumping technology. They explore the economic practicality of solar water pumping systems and identify the gaps in research and the hindrances in the widespread implementation of this technology. The objective of [17] is to create a dynamic modeling tool that integrates the water demand, solar PV power, and pumping system models to check whether an optimal alignment between water demand and supply in PV water pumping systems exists. In [18], the authors investigate the ideal configuration for a PV system that can power a solar submersible pump to meet the domestic water demands of five isolated households in a remote region of Morocco. They also propose a comprehensive approach for designing an optimized PV water pumping system based on actual water usage data. In [19] a water pumping system powered by a hybrid generator comprising both PV and wind energy sources is proposed. That system employs centrifugal pumps driven by variable speed IM that are controlled using a FOC method.

Moreover, the advent of IoT technology has generated a vast potential for innovative methods and smart solutions that can revolutionize the agricultural sector [20]. One of the prominent approaches to smart farming is the use of smart greenhouse farming. There, an enclosed cultivation process that leverages information and communication technology to improve the quality and quantity of crops with minimal human intervention is employed [21, 22]. Therefore, IoT can transform a greenhouse into a smart and automated place, which may assist growers in enhancing the productivity of food and crops [23, 25].

Numerous scientific attempts have been made to advance the application of smart technologies in agricultural practices, specifically in hydroponic greenhouses. One illustrative case is outlined in [23]. The authors develop a smart hydroponic and aeroponic system with advanced sensors and devices for the monitoring of various meteorological parameters inside and outside the agricultural greenhouse. In [24, 25], the authors propose a circulation-free drip hydroponic system adopting IoT technology for pepper plants, which are among the most vitamin-rich vegetables and provide an excellent opportunity for local and export markets. Recently, smart, and remotely connected agricultural greenhouses, which incorporate sustainable development architecture, have emerged. For example, the prototype described in [26, 27] presents a connected hydroponic system that allows users to remotely monitor environmental and plant conditions in order to optimize plant growth.

This study discusses the development and implementation of a smart PV water pumping system designed to regulate the indoor environment of a hydroponic greenhouse ensuring optimum performance. The PV Hydroponic Greenhouse (PV-HG) system regulates the circulation of the hot or cold water to maintain the required temperature for optimal plant growth. It consists of a PV Generator (PVG), a boost DC/DC converter, a three-phase voltage source inverter, an induction motor, a centrifugal pump, and a hydroponic greenhouse.

II. METHODS AND MATERIALS

A. *Description of the Proposed PV-HG*

The schematic diagram illustrated in Figure 1 provides an overview of the configuration of the proposed PV-HG, which is composed of a PVG, a boost DC/DC converter, a DC-bus, a three-phase voltage source inverter, an IM, a Centrifugal Pump (CP), and a Hydroponic Greenhouse (HG).

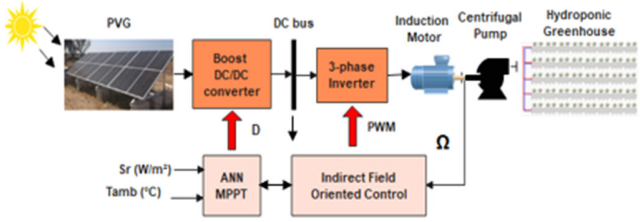

Fig. 1. The schematic diagram of the proposed PV-HG.

B. Modeling of the PVG

The model of a PVG composed of N_p parallel panels with N_s series cells is given by (1):

$$I_{pv} = N_p I_{sc} - N_p I_s \left[exp\left(\left(V_{pv} + R_S I_{pv} \right) / N_s V_T \right) - 1 \right] - \frac{V_{pv} + R_S I_{pv}}{R_p} \quad (1)$$

where I_{pv} (A), V_{pv} (V) are the PV current and voltage respectively, I_s (A) is the diode current, R_s (Ω), R_p (Ω) are the PV array series and parallel resistors, I_{sc} (A) is the short-circuit current, A the panel ideality factor, and $V_T = AKT/q$.

C. Modeling of the Boost DC/DC converter

Typically, the PV voltage V_{pv} is lower than the DC-bus voltage V_{dc} to which the load is connected. Therefore, a boost DC/DC converter is used to match the V_{pv} with the V_{dc}. Figure 2 gives the schematic diagram of the boost DC/DC converter.

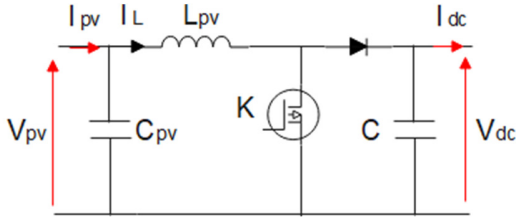

Fig. 2. Schematic diagram of the boost DC/DC converter.

The dynamic model of the boost DC/DC converter is given by (2):

$$\begin{cases} \frac{dV_{pv}}{dt} = \frac{1}{C_{pv}} \left(I_{pv} - I_L \right) \\ \frac{dI_L}{dt} = \frac{1}{L_{pv}} \left((D-1) V_{dc} + V_{pv} \right) \\ \frac{dV_{dc}}{dt} = \frac{1}{C} \left((1-D) I_L - I_{dc} \right) \end{cases} \quad (2)$$

where D is the duty cycle of the boost DC/DC converter.

D. Modeling of the Three-phase Voltage Source Inverter

The DC energy produced by the PVG is converted into AC energy by a three-phase voltage source inverter having three independent branches. Each branch consists of two switches, and each switch is made with a bipolar transistor with an antiparallel diode. The switch control signals of the inverter (*K1, K2, K3*) govern the modulation process. The inverter output voltages (V_{s1}, V_{s2}, V_{s3}) are modulated and expressed by (3):

$$\begin{pmatrix} V_{S1} \\ V_{S2} \\ V_{S3} \end{pmatrix} = \frac{V_{dc}}{3} \begin{pmatrix} 2 & -1 & -1 \\ -1 & 2 & -1 \\ -1 & -1 & 2 \end{pmatrix} \begin{pmatrix} K_1 \\ K_2 \\ K_3 \end{pmatrix} \quad (3)$$

To maintain a balance between the PV and the induction motor power, it is crucial to employ a DC-bus so as $I_c = C \frac{dV_{dc}}{dt}$ where I_c (A) is the DC-bus current.

E. Modeling of the Induction Motor

The electrical model of the induction motor is given by:

$$\begin{cases} I_{ds} = \frac{1}{r_s + \sigma L_s s} \left[V_{ds} - \frac{M}{L_r} s \Phi_{dr} + \frac{\omega_s}{L_r} M \Phi_{qr} + \omega_s \sigma L_s I_{qs} \right] \\ I_{qs} = \frac{1}{r_s + \sigma L_s s} \left[V_{qs} - \frac{M}{L_r} s \Phi_{qr} - \frac{\omega_s}{L_r} M \Phi_{dr} - \omega_s \sigma L_s I_{ds} \right] \\ \Phi_{dr} = \frac{1}{T_r s + 1} \left[T_r (\omega_s - \omega_r) \Phi_{qr} + M I_{ds} \right] \\ \Phi_{qr} = \frac{1}{T_r s + 1} \left[-T_r (\omega_s - \omega_r) \Phi_{dr} + M I_{qs} \right] \end{cases} \quad (4)$$

The mechanical model is given by:

$$\frac{d\omega_r}{dt} = \frac{p^2 M}{J L_r} \left[\Phi_{dr} I_{qs} - \Phi_{qr} I_{ds} \right] - \frac{p}{J} C_r \quad (5)$$

where I_{ds} and I_{qs} correspond to the stator currents, V_{ds} and V_{qs} to the stator voltages, Φ_{dr} and Φ_{qr} are d and q-axis components of the rotor flux, ω_s is the stator angular frequency, ω_r is the electrical rotor speed, R_s, R_r are the stator and rotor resistors, L_s, L_r are the stator and rotor inductances, σ is the viscous friction coefficient, M is the mutual inductance, J corresponds to the rotor inertia moment, p is the number of pole pairs and C_r is the motor load torque.

F. Modeling of the Centrifugal Water Pump

The centrifugal pump is designed to facilitate the circulation of hot or cold water based on both the specific requirements of the plant and seasonal changes. The pump is engineered to harness centrifugal force to transfer water from one location to another, making it an efficient and reliable solution for water circulation. The torque that must be applied to the pump shaft, neglecting mechanical and hydraulic frictions is given by (6):

$$C_r = \frac{W}{2\pi g} Q (\mu_0 N - \lambda_1 Q) \quad (6)$$

where μ_0 and λ_1 are constants depending on pump wheel dimensions. They are calculated from the characteristic of the power supplied to the pump shaft as a function of the flow $P = f(Q)$, at constant speed. W is the liquid density (daN/m^3), Q is the pump flow rate (m^3/s), N is the motor rotation speed (tr/min) and g = 9.81 m/s² is the acceleration of gravity. The power P applied to the shaft is given by (7) as:

$$P = C_r \omega_r = \frac{W}{g} N Q (\mu_0 N - \lambda_1 Q) \quad (7)$$

Furthermore, at the operating mode, the net height of the pump H_n, can be expressed as:

$$H_n = \mu N^2 + \lambda N Q + k Q^2 \quad (8)$$

where μ, λ, and k are constants depending on the pump characteristics. For each speed regime, the efficiency η is given by (9):

$$\eta = \frac{W}{100P} Q H_n \quad (9)$$

This equation makes it possible to calculate, for a rotation speed N provided by the asynchronous motor, the value of the optimal flow rate Q_{opt} corresponding to the pump's optimal efficiency. Therefore, the optimal flow rate is calculated by:

$$Q_{opt} = \frac{\mu_0 k + \sqrt{(\mu_0 k)^2 + k \lambda_1 (\lambda \mu_0 + \lambda_1 \mu)}}{k \lambda_1} N \quad (10)$$

G. Modeling of the Hydroponic Greenhouse

The internal microclimate of the hydroponic greenhouse depends on solar radiation, temperature, relative humidity, and CO2 concentration. The hydroponic greenhouse thermal equilibrium model is developed through neglecting several physical phenomena: irradiative heat exchange between walls and roofs; the storage capacity of sandwich panel walls and the roof; the absorptive capacity and heat capacity of the enclosed air; and conductive heat exchange between the interior air, sandwich panel walls, and the roof. This dynamic model consists of four components: the single-wall cover, the internal air, the canopy, and the protected floor as described in Figure 3.

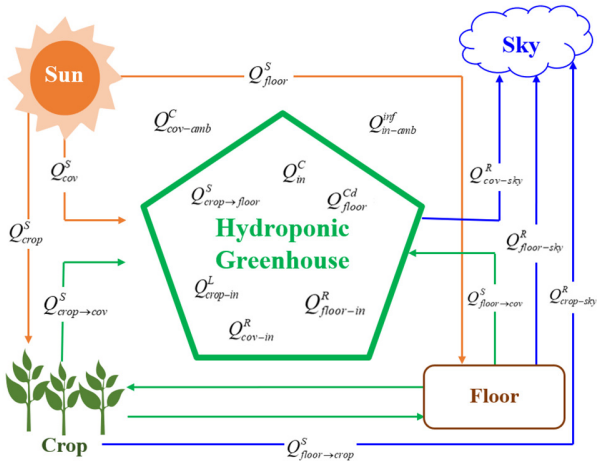

Fig. 3. Schematic representation of the heat flux in hydroponic greenhouse.

In Figure 3, Q^S_{cov}, $Q^S_{crop\to cov}$, $Q^S_{floor\to cov}$, $Q^S_{floor\to crop}$ and Q^S_{floor} correspond to the absorbed heat of the solar energy in all greenhouse components. $Q^C_{cov-amb}$, and Q^C_{in} are the convective heat outside and inside the greenhouse. Q^{Cd}_{floor} is the heat exchanged by conduction from the floor. Q^{inf}_{in-amb} is the heat losses by infiltration. $Q^L_{crop-in}$ is the heat exchanged by evapotranspiration of the crop. $Q^R_{cov-sky}$, ,Q^R_{cov-in}, $Q^R_{crop-in}$, $Q^R_{crop-sky}$, $Q^R_{floor\to in}$, and $Q^R_{floor-sky}$ are the heat losses due to radiation from the greenhouse and its surroundings. Each one of these elements is defined by a state variable, namely the temperature, which is assumed to be uniform across the cover and protected floor surfaces. The indoor air is also characterized by a uniform absolute humidity throughout the entire greenhouse volume. To address this problem, four balance equations have been created for the indoor air of the greenhouse [19].

The heat balance at the cover is given by:

$$\frac{dT_{cov}}{dt} = \frac{1}{d_{air}C_pA_{cov}}\left(Q^S_{cov} + Q^S_{crop\to cov} + Q^S_{floor\to cov} - Q^C_{cov-amb} - Q^C_{in} + Q^R_{cov-sky} + Q^R_{cov-in}\right) \quad (11)$$

where T_{cov} is the coverture temperature, d_{air} is the air density, C_p is the specific heat of air at a constant pressure, A_{cov} is the surface area of the coverture.

The calculation of the crop's energy balance is provided by:

$$\frac{dT_{crop}}{dt} = \frac{1}{d_{air}C_pA_{crop}}\left(Q^S_{crop} + Q^S_{floor\to crop} - Q^R_{crop-in} - Q^R_{crop-sky} - Q^L_{crop-in}\right) \quad (12)$$

where T_{crop} is the crop temperature and A_{crop} is the surface area of the crop.

The calculation of the energy balance at the greenhouse floor gives:

$$\frac{dT_{floor}}{dt} = \frac{1}{d_{air}C_pA_{floor}}\left(Q^S_{floor} - Q^{Cd}_{floor} - Q^R_{floor-in} - Q^R_{floor-sky}\right) \quad (13)$$

where T_{floor} is the floor temperature and A_{floor} is the surface area of the floor.

The dynamic equation describing the thermal evolution of the internal air is given by (14) :

$$\frac{dT_{in}}{dt} = \frac{1}{d_aC_aV}\left(Q^C_{in} - Q^R_{cov-in} - Q^R_{crop-in} - Q^{inf}_{in-amb}\right) \quad (14)$$

where T_{in} is the crop temperature and V the volume of the greenhouse.

H. ANN-based MPPT

The expression of an Artificial Neural Network's (ANN) mathematical model is typically presented as a set of interconnected mathematical equations that define the network's structure and behavior [19]. It allows for the analysis and prediction of the network's output for specific input patterns as in (15):

$$\begin{aligned} a^0 &= p \\ a^i &= f^j(w^j a^{i-1} + b^j) \end{aligned} \quad (15)$$

where p is the input vector, w is the weight, b is the bias, α is the output of the layer, f is the activation function and j is the layer index. During the training process, the ANN models the input-output relationship of a dataset by adjusting the weights to minimize the difference between the network outputs and the desired values. Once the training is completed, the network can predict the output from a given input pattern. During the training process, the connection weights are adjusted until the input-output patterns match with the minimum errors, indicating the best fit. The recommended performance evaluation criterion, in this case, is the Mean Square Error (MSE).

In this study, a two-layer feed-forward ANN architecture is used to track the Maximum Power Points (MPP) and to generate the duty cycle of the converter. It is considered that the input layer is composed of a solar radiation S_r and an ambient temperature T_{amb}. Furthermore, the output layer is associated with V_{mpp}, i.e. the optimal voltage of the PVG. The training dataset included 70% of the total samples, whereas the cross-validation and testing datasets contained 15% of the samples. V_{mpp} was then compared with V_{pv} and the error was compensated with a discrete PID controller that generated the appropriate duty cycle of the boost DC/DC converter, as portrayed in Figure 4.

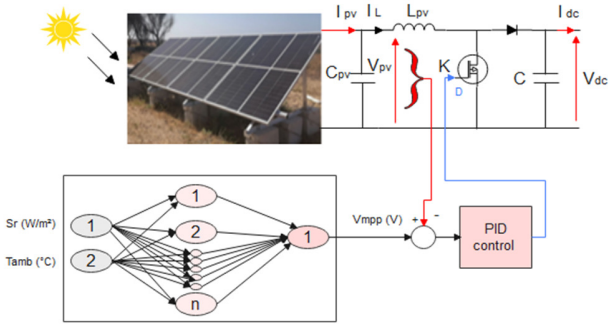

Fig. 4. The architecture of the ANN-based MPPT controller.

I. Indirect Field-Oriented Control of the Induction Motor

For the Indirect Field-Oriented Control (IFOC), the Park angle was calculated from the stator pulsation. The pulsation was reconstituted using the speed of the machine and its rotor to control the stator current and subsequently fix its operating point. The IFOC is based on the orientation of the Park referential such that the q-axis component of the rotor flux is zero as in (16):

$$\begin{cases} \Phi_{dr} = \Phi_r \\ \Phi_{qr} = 0 \end{cases} \quad (16)$$

Therefore, the model of the IFOC is given by (17):

$$\begin{cases} V_{ds} = R_s I_{ds} + \sigma L_s \frac{dI_{ds}}{dt} - \omega_s \sigma L_s I_{qs} \\ V_{qs} = R_s I_{qs} + \sigma L_s \frac{dI_{qs}}{dt} + \omega_s \sigma L_s I_{ds} \\ \Phi_r = M I_{ds} \\ \omega_s = \omega_r + \frac{M I_{qs}}{T_r \Phi_r} \end{cases} \quad (17)$$

The electromagnetic torque of the IM is expressed by (18):

$$C_{em} = (3pM/2L_r)\Phi_r I_{qr} \quad (18)$$

The structure of the proposed IFOC based on the optimized ANN-PID controller is outlined in Figure 5. The reference values of rotor flux and currents are calculated by:

$$\begin{cases} \Phi_r^*(\Omega) = \sqrt{3}\frac{L_r V_{sn}}{M \omega_{sb}} \; if \; \Omega \le \Omega_b \\ \Phi_r^*(\Omega) = 2\frac{P L_r}{3pM} \; if \; \Omega > \Omega_b \end{cases} \quad (19)$$

$$\begin{cases} I_{ds}^* = \frac{\Phi_r^*}{M} \\ I_{qs}^* = C_{em}^* / \left[\left(\frac{3pM}{2L_r}\right)\Phi_r^*\right] \end{cases} \quad (20)$$

By neglecting friction and the losses of the induction motor, the power can be expressed according to the load torque and speed as follows:

$$P \approx C_r \omega_r \approx= A_p {\omega_r}^3 \quad (21)$$

where A_p is the torque constant of the induction motor. Then, (22) represents the reference speed of the induction motor, which corresponds to the optimal PV power (P_{opt}) generated by the PVG:

$$\Omega^* = \sqrt[3]{\frac{P_{opt}}{A_p}} \quad (22)$$

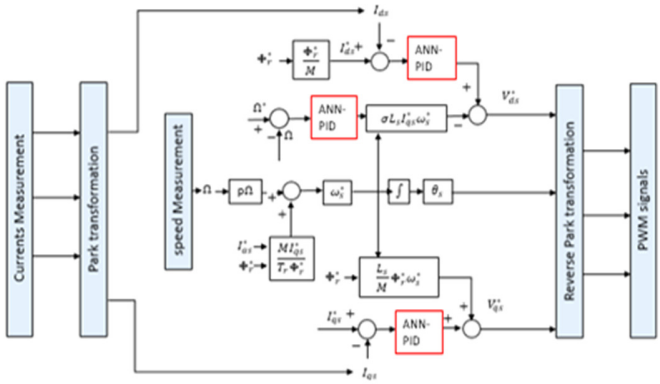

Fig. 5. The synoptic diagram of the IFOC of the induction motor.

III. SIMULATION AND EXPERIMENTAL RESULTS

A. Simulation Results of the PV-HG

This system was implemented in Simulink-Matlab. Figure 6 displays the variation of solar radiation (I_r) with time.

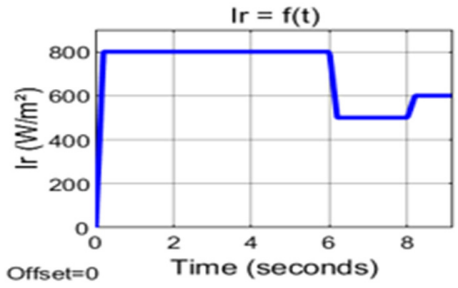

Fig. 6. Solar irradiation waveform.

Consequently, the waveforms of the PV current and the DC-bus voltage are manifested in Figures 7(a) and 7(b). Owing to the ANN-based MPPT developed here, the PV current and the DC-bus voltage were optimally evaluated, which contributes to maximizing the power output of the PV generator.

The IFOC is implemented in Simulink-Matlab and Figures 8(a) and 8(b) demonstrate the waveforms of the mechanical speed N of the centrifugal pump and its flow rate Q, respectively, for the same irradiation simulation variation. For the performance optimization of both the IM and the centrifugal pump, the rotational speed (N) and the flow rate (Q) ultimately converged towards their respective optimal values, signaling a tendency to follow the changes in specific speed (S_r). This phenomenon is a key factor in achieving the maximum efficiency of these machines.

B. Experimental Implementation of a Smart PV-HG

In this study, an IoT-based system for the remote control of the internal and external parameters relevant to plant growth is designed and implemented in a hydroponic greenhouse. These parameters are lighting, internal and external temperature, relative humidity, soil moisture, and water flow rate. The IoT system consists of a sensor network and an ESP32 microcontroller. The information provided by the sensors is

transferred to the microcontroller that, in turn, integrates all the data into a single platform, analyzes it, and then decides by remotely interacting with the user via the internet, the optimal way forward. The Wi-Fi connection with the cloud allows the recorded data to be transmitted and stored in databases.

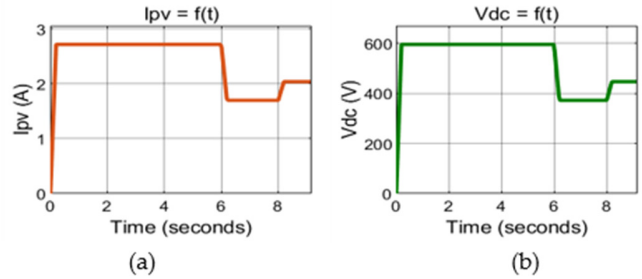

Fig. 7. PV-current (a) and DC-bus voltage (b) waveforms.

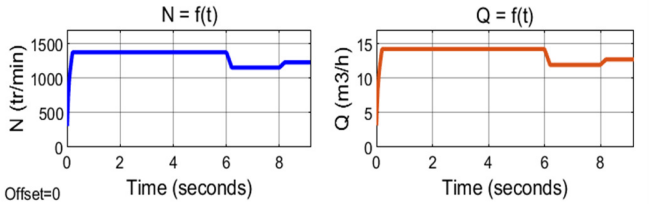

Fig. 8. The mechanical speed (a) and the flow rate (b) waveforms.

C. Sensor Network

Temperature is one of the primary environmental factors that affect plant growth and development. The ideal temperature range for most plants is between 65 - 75 °F (18 - 24 °C) [20]. Temperatures outside of this range can cause stress to the plants and affect their growth rate and overall health. High temperatures can generate wilting and dehydration, whereas low temperatures can slow down growth and even cause damage to the plant's tissues. Therefore, maintaining the ideal temperature range is crucial for optimal plant growth and development. A DHT11 sensor is deployed to measure the ambient temperature inside and outside the greenhouse. To maintain optimal humidity levels inside the greenhouse and ensure that the plant receives the right amount of moisture, a soil humidity sensor SEN-13322 is utilized for regular monitoring and control. Additionally, lighting is another crucial factor in promoting rapid photosynthesis for plant growth. It is interesting to note that the control of light intensity inside a greenhouse can be provided by an LDR sensor. This sensor consists of a photoconductive cell that is covered with a moisture-resistant coating and safely put in a plastic housing. The best part is that the lighting intensity can be automatically adjusted, which is a great way to ensure that the plants get the right amount of light throughout the day. Finally, the water flow rate is measured via an YF-S201 sensor.

Thus, the complete sensor network is composed of a DHT11 sensor for measuring the temperature and relative humidity, an LDR sensor for measuring the light intensity, a soil moisture sensor SEN-13322, and a flow meter YF-S201 for measuring the pumped water flow. The microcontroller employed in this study is of an ESP32 type because of its many advantages, involving low-power programming and Wi-fi capabilities. Figure 9 illustrates the smart PV-HG equipped with all the IoT sensors and the ESP32. The implementation of the smart system into the hydroponic greenhouse is depicted in Figure 10.

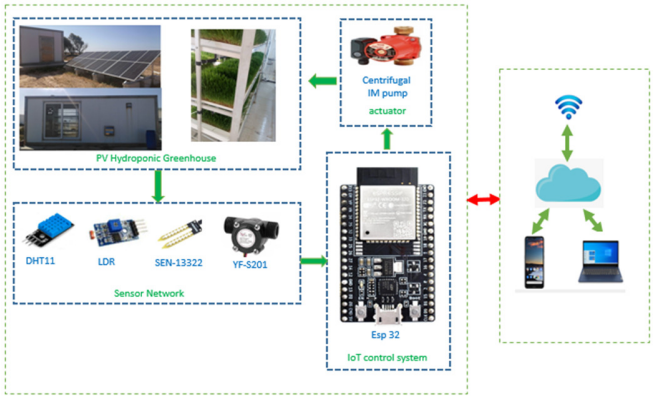

Fig. 9. The smart PV-HG.

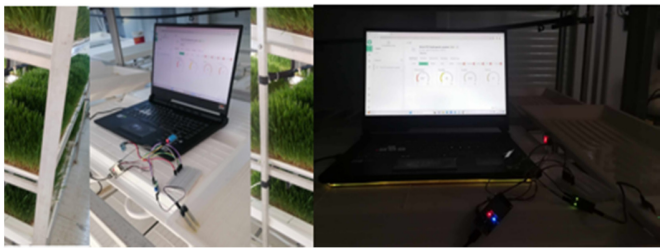

Fig. 10. Implementation of the smart IoT-based PV-HG.

The Blynk console platform offers an easy-to-use solution for developing web applications that can collect and visualize data from sensors. This platform provides a comprehensive set of tools to create a custom graphical user interface that can display real-time sensor measurements. The web application developed engaging the Blynk console platform, exhibited in Figure 11, enables users to collect and store data from various sensors in a structured manner. These data can then be accessed and analyzed for various purposes.

The IoT system has meticulously gathered and recorded the precise values of solar radiation, ambient temperature, and IM power consumption over a span of six days in June 2023 in Tunisia. This comprehensive and accurate dataset is presented in a clear and concise manner in Figure 12, allowing for easy analysis and interpretation.

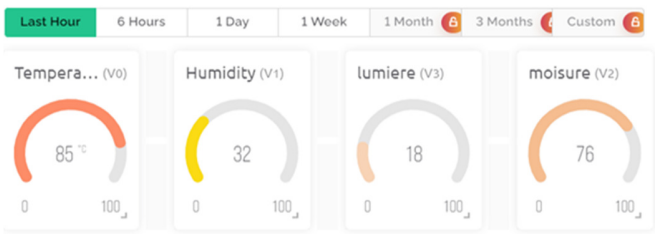

Fig. 11. Web application for the smart PV-HG parameters controlling.

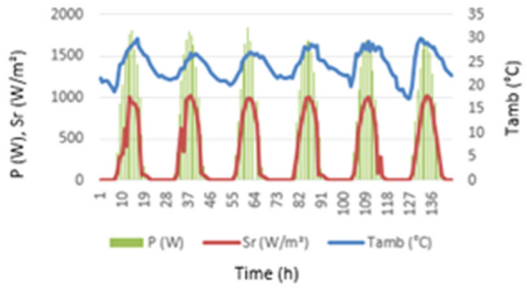

Fig. 12. Measurements of solar radiation, ambient temperature, and power consumption of the PV-HG for 6 days in June 2023 in Tunisia.

The changes in the IM power and water flow rate of the centrifugal pump were observed for a single day. The corresponding variations are portrayed in Figures 13 and 14.

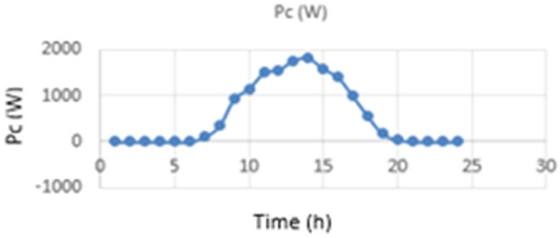

Fig. 13. Measurements of the Power consumption for one day in June 2023.

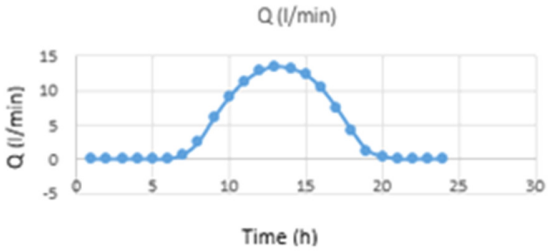

Fig. 14. Measurements of the water flow rate for one day in June 2023.

The water flow rate varies according to the climatic conditions, and this variation can be optimized to achieve the best performance of the system. The proposed control strategies, which use an ANN-based MPPT and IFOC, have proven effective in tracking the MPP and optimizing the IM performance. These results demonstrate the potential of the deployed control strategies in enhancing the overall performance of the system.

During the specific time frame mentioned, the cooling and heating temperatures of the hydroponic greenhouse have been recorded. These measurements have been meticulously analyzed and compiled into easy-to-understand visual representations in Figures 15 and 16. The information provided in these figures can be exploited to gain a better understanding of the temperature conditions within the greenhouse during this period.

It is evident that the actual temperature is in line with the reference temperature necessary for optimal plant growth. This indicates that the PV-HG system has been successful in maintaining optimal indoor conditions for the microclimate of the plant.

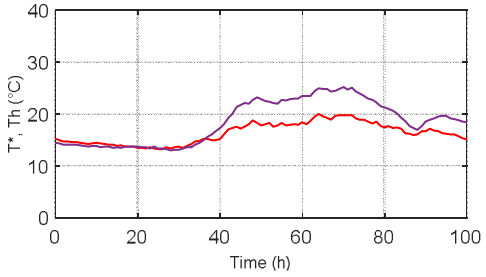

Fig. 15. Measurements of the heating temperature versus the required temperature in the HG.

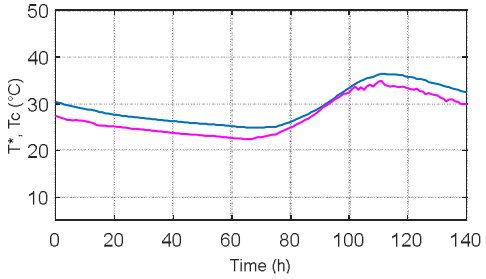

Fig. 16. Measurements of the cooling temperature versus the required temperature in the HG.

IV. CONCLUSIONS

This paper proposes a smart hydroponic greenhouse system that uses solar energy for irrigation, water pumping, and crop and indoor climate management regardless of the weather fluctuations. To achieve this, the system implements MPPT control, based on an ANN, which continuously monitors and extracts the maximum amount of energy from the solar source. In addition, the system deploys field-oriented indirect control based on optimized ANN-PID controllers to adjust the speed of the pump. This helps maintain water flow in the system and certifies that the water temperature is always at the optimal value for the plants. Additionally, an IoT-based system for remote control of important plant growth parameters is designed and implemented in a hydroponic greenhouse. It includes a sensor network and an ESP32 microcontroller, which integrate data into a single platform. The system analyzes data and interacts with the user via Wi-Fi to remotely control lighting, temperature, humidity, soil moisture and water flow. The system also records and stores data in databases through cloud connectivity. The experimental results proved the effectiveness of the proposed PV-HG in regulating the microclimate of the agricultural farm.

This approach offers several advantages over traditional greenhouse growing methods. Initially, the use of IoT enables precise and automated microclimate control, leading to better agricultural yields and improved resource efficiency. It allows dynamic adjustments based on real-time data, ensuring optimal growing conditions for plants. Second, the integration of

photovoltaic energy systems provides a sustainable and renewable energy source, reducing dependence on traditional energy networks while minimizing the environmental impact of greenhouse operations. The combination of IoT, hydroponics and renewable energy sources, particularly PVs, provides better results on cost, crop quality and the environment.

ACKNOWLEDGMENT

The authors especially thank the ATSSEE, the Physics Department of the Faculty of Science of Tunis, the Research and Technology Center of Energy of Bordj-Cedria, Tunisia, the Ministry of Higher Education and Scientific Research, and the University of French Guiana, UMR Espace-Dev, Cayenne, French Guiana for the excellent communication, information collection and funding provision during the implementation of this study.

REFERENCES

[1] X. Zhang, G. Manogaran, and B. Muthu, "IoT enabled integrated system for green energy into smart cities, " Sustainable Energy Technologies and Assessments, vol. 46, Aug. 2021, Art no. 101208, https://doi.org/10.1016/j.seta.2021.101208.

[2] G. Wu, H. Fang, Y. Zhang, K. Li, and D. Xu, "Photothermal and Photovoltaic Utilization for Improving the Thermal Environment of Chinese Solar Greenhouses: A Review, " *Energies*, vol. 16, no. 19, Jan. 2023, Art. No. 6816, https://doi.org/10.3390/en16196816.

[3] I. Ullah, N. Khan, Y. Dai, and A. Hamza, "Does Solar-Powered Irrigation System Usage Increase the Technical Efficiency of Crop Production? New Insights from Rural Areas," *Energies*, vol. 16, no. 18, Jan. 2023, Art. No. 6641, https://doi.org/10.3390/en16186641.

[4] N. Sadek, N. kamal, and D. Shehata, "Internet of Things based smart automated indoor hydroponics and aeroponics greenhouse in Egypt," *Ain Shams Engineering Journal*, vol. 15, no. 2, Feb. 2024, Art. No. 102341, https://doi.org/10.1016/j.asej.2023.102341.

[5] F. M. Ribeiro Junior, R. A. C. Bianchi, R. C. Prati, K. Kolehmainen, J.-P. Soininen, and C. A. Kamienski, "Data reduction based on machine learning algorithms for fog computing in IoT smart agriculture," *Biosystems Engineering*, vol. 223, pp. 142–158, Nov. 2022, https://doi.org/10.1016/j.biosystemseng.2021.12.021.

[6] N. Ra, A. Ghosh, and A. Bhattacharjee, "IoT-based smart energy management for solar vanadium redox flow battery powered switchable building glazing satisfying the HVAC system of EV charging stations,"*Energy Conversion and Management*, vol. 281, Apr. 2023, Art. No. 116851, https://doi.org/10.1016/j.enconman.2023.116851.

[7] D. Hidouri, R. Marouani, and A. Cherif, "Modeling and Simulation of a Renewable Energy PV/PEM with Green Hydrogen Storage,"*Engineering, Technology & Applied Science Research*, vol. 14, no. 1, pp. 12543–12548, Feb. 2024, https://doi.org/10.48084/etasr.6492.

[8] G. Msigwa, J. O. Ighalo, and P.-S. Yap, "Considerations on environmental, economic, and energy impacts of wind energy generation: Projections towards sustainability initiatives," *Science of The Total Environment*, vol. 849, Nov. 2022, Art. No. 157755, https://doi.org/10.1016/j.scitotenv.2022.157755.

[9] J. Morales-García *et al.*, "SEPARATE: A tightly coupled, seamless IoT infrastructure for deploying AI algorithms in smart agriculture environments," *Internet of Things*, vol. 22, Jul. 2023, Art. No. 100734, https://doi.org/10.1016/j.iot.2023.100734.

[10] A. I. Montoya-Munoz, R. A. C. da Silva, O. M. C. Rendon, and N. L. S. da Fonseca, "Reliability provisioning for Fog Nodes in Smart Farming IoT-Fog-Cloud continuum, " *Computers and Electronics in Agriculture*, vol. 200, Sep. 2022, Art. No. 107252, https://doi.org/10.1016/j.compag.2022.107252.

[11] C. Maraveas, D. Piromalis, K. G. Arvanitis, T. Bartzanas, and D. Loukatos, "Applications of IoT for optimized greenhouse environment and resources management," *Computers and Electronics in Agriculture*, vol. 198, Jul. 2022, Art. No. 106993, https://doi.org/10.1016/j.compag.2022.106993.

[12] V. Mamatha and J. C. Kavitha, "Machine learning based crop growth management in greenhouse environment using hydroponics farming techniques," *Measurement: Sensors*, vol. 25, Feb. 2023, Art. No. 100665, https://doi.org/10.1016/j.measen.2023.100665.

[13] D. L. Lemes *et al.*, "Estimation of Electrical Energy Consumption in Irrigated Rice Crops in Southern Brazil," *Energies*, vol. 16, no. 18, Jan. 2023, Art. No. 6742, https://doi.org/10.3390/en16186742.

[14] H. S. A. Lagili, A. Kiraz, Y. Kassem, and H. Gökçekuş, "Wind and Solar Energy for Sustainable Energy Production for Family Farms in Coastal Agricultural Regions of Libya Using Measured and Multiple Satellite Datasets," *Energies*, vol. 16, no. 18, Jan. 2023, Art. No. 6725, https://doi.org/10.3390/en16186725.

[15] A. I. Khan, F. Alsolami, F. Alqurashi, Y. B. Abushark, and I. H. Sarker, "Novel energy management scheme in IoT enabled smart irrigation system using optimized intelligence methods," *Engineering Applications of Artificial Intelligence*, vol. 114, Sep. 2022, Art. No. 104996, https://doi.org/10.1016/j.engappai.2022.104996.

[16] G. Kaur, P. Upadhyaya, and P. Chawla, "Comparative analysis of IoT-based controlled environment and uncontrolled environment plant growth monitoring system for hydroponic indoor vertical farm," *Environmental Research*, vol. 222, Apr. 2023, Art. No. 115313, https://doi.org/10.1016/j.envres.2023.115313.

[17] K. Kaczmarczyk, P. Dobrzaniecki, M. Woszczyński, D. Bałaga, K. Szewerda, and A. Dymarek, "Wind Power Plants and Selected Technical and Economic Aspects of Their Construction on Mine Heaps," *Energies*, vol. 16, no. 19, Jan. 2023, Art. No. 6827, https://doi.org/10.3390/en16196827.

[18] A. A. Junior, T. J. A. da Silva, and S. P. Andrade, "Smart IoT lysimetry system by weighing with automatic cloud data storage," *Smart Agricultural Technology*, vol. 4, Aug. 2023, Art. No. 100177, https://doi.org/10.1016/j.atech.2023.100177.

[19] F. Jamil, M. Ibrahim, I. Ullah, S. Kim, H. K. Kahng, and D.-H. Kim, "Optimal smart contract for autonomous greenhouse environment based on IoT blockchain network in agriculture," *Computers and Electronics in Agriculture*, vol. 192, Jan. 2022, Art. No. 106573, https://doi.org/10.1016/j.compag.2021.106573.

[20] M. García-Monge *et al.*, "Is IoT monitoring key to improve building energy efficiency? Case study of a smart campus in Spain, " *Energy and Buildings*, vol. 285, Apr. 2023, Art. No. 112882, https://doi.org/10.1016/j.enbuild.2023.112882.

[21] A.-M. N. Dimitropoulou, V. Z. Maroulis, and E. N. Giannini, "A Simple and Effective Model for Predicting the Thermal Energy Requirements of Greenhouses in Europe," *Energies*, vol. 16, no. 19, Jan. 2023, Art. No. 6788, https://doi.org/10.3390/en16196788.

[22] F. Cepolina, F. Silenzi, L. Cirillo, C. Schenone, and M. Zoppi, "Energizing Sustainable Agriculture: Advances in Greenhouse Heating through Microwave-Based Technologies, " *Energies*, vol. 16, no. 23, Jan. 2023, Art. No. 7843, https://doi.org/10.3390/en16237843.

[23] A. Castañeda-Miranda and V. M. Castaño-Meneses, "Smart frost measurement for anti-disaster intelligent control in greenhouses via embedding IoT and hybrid AI methods, " *Measurement*, vol. 164, Nov. 2020, Art. No. 108043, https://doi.org/10.1016/j.measurement.2020.108043.

[24] H. Andrianto, Suhardi, and A. Faizal, "Development of Smart Greenhouse System for Hydroponic Agriculture," in *2020 International Conference on Information Technology Systems and Innovation (ICITSI)*, 2020, pp. 335–340, https://doi.org/10.1109/ICITSI50517.2020.9264917.

[25] S. Al-Naemi and A. Al-Otoom, "Smart sustainable greenhouses utilizing microcontroller and IOT in the GCC countries; energy requirements & economical analyses study for a concept model in the state of Qatar," *Results in Engineering*, vol. 17, Mar. 2023, Art. No. 100889, https://doi.org/10.1016/j.rineng.2023.100889.

[26] A. Lachheb, R. Marouani, C. Mahamat, S. Skouri, and S. Bouadila, "Fostering Sustainability through the Integration of Renewable Energy in an Agricultural Hydroponic Greenhouse," *Engineering, Technology &*

Applied Science Research, vol. 14, no. 2, pp. 13398–13407, Apr. 2024, https://doi.org/10.48084/etasr.6939.

[27] Y. Kassem, H. Camur, M. T. Adamu, T. Chikowero, and T. Apreala, "Prediction of Solar Irradiation in Africa using Linear-Nonlinear Hybrid Models," *Engineering, Technology & Applied Science Research*, vol. 13, no. 4, pp. 11472–11483, Aug. 2023, https://doi.org/10.48084/etasr.6131.